

Article

Oral Immunization with rVSV Bivalent Vaccine Elicits Protective Immune Responses, Including ADCC, against Both SARS-CoV-2 and Influenza A Viruses

Maggie Jing Ouyang ^{1,2}, Zhujun Ao ^{1,2}, Titus A. Olukitibi ^{1,2}, Peter Lawrynuik ¹, Christopher Shieh ¹, Sam K. P. Kung ³, Keith R. Fowke ², Darwyn Kobasa ^{2,4} and Xiaojian Yao ^{1,2,*}

- ¹ Laboratory of Molecular Human Retrovirology, Department of Medical Microbiology and Infectious Diseases, Max Rady College of Medicine, Rady Faculty of Health Sciences, University of Manitoba, 508-745 Bannatyne Ave, Winnipeg, MB R3E 0J9, Canada; jing.ouyang@umanitoba.ca (M.J.O.); zhujun.ao@umanitoba.ca (Z.A.); olukitit@myumanitoba.ca (T.A.O.); lawrynup@myumanitoba.ca (P.L.); chris.shieh.sen@gmail.com (C.S.)
- ² Department of Medical Microbiology and Infectious Diseases, Max Rady College of Medicine, Rady Faculty of Health Sciences, University of Manitoba, 745 Bannatyne Ave, Winnipeg, MB R3E 0J9, Canada; keith.fowke@umanitoba.ca (K.R.F.); darwyn.kobasa@phac-aspc.gc.ca (D.K.)
- ³ Department of Immunology, Max Rady College of Medicine, Rady Faculty of Health Sciences, University of Manitoba, Winnipeg, MB R3E 0W3, Canada; sam.kung@umanitoba.ca
- ⁴ Special Pathogens Program, National Microbiology Laboratory, Public Health Agency of Canada, Winnipeg, MB R3E 3L5, Canada
- * Correspondence: xiao-jian.yao@umanitoba.ca

Abstract: COVID-19 and influenza both cause enormous disease burdens, and vaccines are the primary measures for their control. Since these viral diseases are transmitted through the mucosal surface of the respiratory tract, developing an effective and convenient mucosal vaccine should be a high priority. We previously reported a recombinant vesicular stomatitis virus (rVSV)-based bivalent vaccine (v-EM2/SPΔC1_{Delta}) that protects animals from both SARS-CoV-2 and influenza viruses via intramuscular and intranasal immunization. Here, we further investigated the immune response induced by oral immunization with this vaccine and its protective efficacy in mice. The results demonstrated that the oral delivery, like the intranasal route, elicited strong and protective systemic immune responses against SARS-CoV-2 and influenza A virus. This included high levels of neutralizing antibodies (NAbs) against SARS-CoV-2, as well as strong anti-SARS-CoV-2 spike protein (SP) antibody-dependent cellular cytotoxicity (ADCC) and anti-influenza M2 ADCC responses in mice sera. Furthermore, it provided efficient protection against challenge with influenza H1N1 virus in a mouse model, with a 100% survival rate and a significantly low lung viral load of influenza virus. All these findings provide substantial evidence for the effectiveness of oral immunization with the rVSV bivalent vaccine.

Keywords: COVID-19; oral immunization; bivalent vaccine; vesicular stomatitis virus (VSV); VSV vector; SARS-CoV-2; influenza virus; neutralizing antibody; ADCC activity



Citation: Ouyang, M.J.; Ao, Z.; Olukitibi, T.A.; Lawrynuik, P.; Shieh, C.; Kung, S.K.P.; Fowke, K.R.; Kobasa, D.; Yao, X. Oral Immunization with rVSV Bivalent Vaccine Elicits Protective Immune Responses, Including ADCC, against Both SARS-CoV-2 and Influenza A Viruses. *Vaccines* **2023**, *11*, 1404. <https://doi.org/10.3390/vaccines11091404>

Academic Editor: Seik-Soon Khor

Received: 26 July 2023

Revised: 14 August 2023

Accepted: 21 August 2023

Published: 23 August 2023



Copyright: © 2023 by the authors. Licensee MDPI, Basel, Switzerland. This article is an open access article distributed under the terms and conditions of the Creative Commons Attribution (CC BY) license (<https://creativecommons.org/licenses/by/4.0/>).

1. Introduction

The global battle against the COVID-19 pandemic has lasted for three years. Waves of emerging variants break through the protection obtained from previous vaccination or infection [1]. Although COVID-19 vaccines attenuate illness severity [1,2], there are still significant numbers of new cases and deaths worldwide [3]. Improving vaccine efficiency is a top priority for effective COVID-19 control. The limitations of the current SARS-CoV-2 vaccines include a spike protein (SP or S) antigen that has become highly mutated, as well as an intramuscular immunization route, which lacks a protection that is strong and specific to the respiratory tract [4,5]. It has been reported that following a booster of the

Pfizer COVID-19 vaccine (i.m.), salivary mucosal immunity against the Wuhan strain relied on serum-exuded IgG, but not on locally produced secretory IgA, because the vaccine failed to activate an effective mucosal immunity [5]. Influenza is another important respiratory infectious disease causing a high disease burden. Influenza control faces similar problems annually: unpredictable prevailing strains and limited protection from intramuscular vaccines.

The natural portal of entry for SARS-CoV-2 and the influenza virus is the mucous membranes lining the respiratory tract, including the nose, mouth, trachea, and lungs [6,7]. Therefore, the mucosa is the first line of defense against viruses. Further, the protective mucosal immune responses (the production of secretory IgA) have been reported to occur earlier than the systemic antibodies during their infection [8]. Theoretically, mucosal vaccines administered via the respiratory tract may elicit more robust local protective immune responses in comparison to intramuscular vaccines. Previous mice and macaque studies have reported that intranasal COVID-19 vaccines induced robust mucosal and systemic immune responses, especially tissue-resident memory T and B cells [9,10]. The immunized animals were completely protected against lethal SARS-CoV-2 challenge. Moreover, viral replication was not detected in the airways and lungs of immunized animals following viral challenge [9,10]. Recently, four mucosal COVID-19 vaccines have been approved for human emergency use, and about 20 mucosal vaccines have reached clinical trials in humans [11–14]. The approved vaccines from China (CanSino Biologics), India (Bharat Biotech), Iran (Razi Vaccine and Serum Res), and Russia (Sputnik V) are adenovirus vectored. The CanSino vaccine is an aerosolized mist inhaled orally through the nose and mouth [15,16] The Bharat vaccine is administered via nose drops [12] The Iranian (Razi Vaccine and Serum Res) and Russian (Sputnik V) vaccines both are nasal sprays [11,12,17] Oral vaccines, as one type of mucosal vaccine, can be easily administered to the mouth or gut without any device (such as a sprayer for the intranasal vaccine). They can successfully induce immune responses since the antigens can easily reach lymphatic tissues including the tonsils or adenoid in the mouth as well as the Peyer's patches or solitary lymphatic nodules in the gut. For example, Vaxart's oral tablet COVID-19 vaccine that targets the mucosal epithelium of the small bowel has been demonstrated to generate broad cross-reactive T-cell and mucosal IgA responses in a phase I clinical trial [14].

The mucosal delivery of recombinant vesicular stomatitis virus (rVSV) has been an interesting area of research. The rVSV vaccine vector is a promising platform with some favorable characteristics, including its non-pathogenic nature and low pre-existing immunity in humans [18]. The replacement of VSV-glycoprotein (G) with a viral antigen from the virus of interest may further reduce its tropism. Importantly, the safety of the rVSV vector has been demonstrated by many animal studies and clinical trials for the rVSV-based Zaire Ebola virus vaccine (VSV-ZEBOV-GP, ERVEBO), which was approved by the FDA for human use in 2019 [19–23] However, the VSV-ZEBOV-GP vaccine was administered intramuscularly. Also, it was reported that when the wild-type VSV is administered intranasally, its neurotoxicity is still a concern because it carries the potential for brain infection via the olfactory tract above the nose cavity [24]. While oral delivery of rVSV may carry a smaller risk than the intranasal route, it is worth noting that oral delivery of the rVSV vaccine has been reported to induce protective immune responses against the Sin Nombre virus and SARS-CoV-2 infection [25,26] The rVSV–Sin Nombre virus (SNV) vaccine was delivered to deer mice via oral gavages, in which the SNV glycoprotein (G) replaced the VSV-G to mediate vaccine entry into the mucosa [25,27] The rVSV-SARS2(+G) vaccine targeted the oral cavity mucosa through the VSV-G proteins that were incorporated in the virion's surface (trans-complemented) and were responsible for the target cell tropism [26] We recently have reported a replication-competent rVSV-based bivalent vaccine (v-EM2/SPΔC1_{Delta}) that effectively protected animals against both SARS-CoV-2 and the influenza A virus [28]. This bivalent vaccine has a modified Ebola virus glycoprotein (GP) that mediates rVSV entry to cells, including macrophages and dendritic cells (DCs). Our vaccine has elicited robust adaptive immune responses via either intramuscular or intranasal vaccination in mice or hamsters.

Vaccine-induced virus-specific antibodies provide anti-viral protection through not only neutralization, but also extra-neutralizing functions, such as antibody-dependent cellular cytotoxicity (ADCC), antibody-dependent cellular phagocytosis (ADCP), and complement-dependent cytotoxicity (CDC) [29]. Among them, ADCC has been linked to the resolution of and protection against several viruses, including SARS-CoV-2 [30–34], influenza virus [35,36], HIV-1 [37], and Ebola virus [38]. Yu et al. reported that COVID-19 patients who had recovered from severe disease had greater ADCC activity than patients who had succumbed to severe disease [34]. Vigon et al. discovered that COVID-19 patients who required ICU assistance had significantly enhanced levels of memory B cells, plasmablasts, and neutralizing antibodies against SARS-CoV-2, but also impaired ADCC activity [30]. These findings strongly suggest that ADCC activity should be used to evaluate potential vaccines against SARS-CoV-2 in addition to NABs.

In this study, we investigated the immune responses induced by oral immunization with a rVSV-based bivalent vaccine (v-EM2/SPΔC1_{Delta}) in mice and compared them to intranasal immunization. We found that oral immunization elicited strong systematic immune responses against the Delta variant and influenza H1N1 virus, including neutralizing antibodies (NABs) and antibody-dependent cellular cytotoxicity (ADCC) activity, which were similar to the efficacy of the intranasal immunization route. Further, oral immunization provided complete protection against influenza A H1N1 viral challenge in mice, like the intranasal route, with a 100% survival rate, as well as less weight loss, and alongside significantly lower viral loads in the lungs. In addition, we discovered that the antibodies targeting SP and M2e were positively correlated with ADCC activity against SARS-CoV-2 and influenza.

2. Materials and Methods

2.1. Ethics Statement

The animal experiments described were carried out according to protocols approved by the Central Animal Care Facility, University of Manitoba (Protocol Approval No. 20-034), following the guidelines provided by the Canadian Council on Animal Care. All animals were acclimated for at least one week before experimental manipulations and maintained with food and water ad libitum in a specific pathogen-free animal facility.

2.2. Cells, Plasmids, Antibodies, Recombinant Proteins, Viruses, and Vaccine Production

The HEK293TN cells, human lung type II pulmonary epithelial A549_{ACE2} cell line, and VeroE6 cells were described previously [39,40]. The Madin–Darby canine kidney (MDCK) cell line was described in [41]. Each of these cell lines were cultured in DMEM medium. Jurkat–Lucia NFAT-CD16 cells (Invivogen, Cat# jktl-nfat-cd16, San Diego, CA, USA) were cultured in RPMI-1640 medium. The plasmids pCAGGS expressing SARS-CoV-2 SPΔC (deleted C-terminal 17 aa) from the original strain Wu-Han-1 (SPΔC_{WH}), Delta variant B.1.617.2 (SPΔC_{Delta}), and human influenza A virus M2 were constructed previously [28,39,42]. The antibodies used in this study included rabbit polyclonal antibody against SARS-CoV-2 SP/RBD (Sino Biological, Cat# 40150-R007, Beijing, China), mouse monoclonal anti-SARS-CoV-2 S2 antibody (Abcam, Cat# 1A9: ab273433, Cambridge, UK), human SARS-CoV-2 SP-NTD antibody (Elabscience, Cat# E-AB-V1030, Huston, TX, USA), mouse monoclonal anti-influenza A virus M2 antibody (Santa Cruz Biotech, Cat# 14C2: sc-32238, Dallas, TX, USA), and anti-mouse-HRP antibody (GE Healthcare, Cat# NA931, Chicago, IL, USA). Recombinant proteins included RBD peptide (RayBiotech, Cat# 230-30162, Peachtree Corners, GA, USA), S1 subunit (RayBiotech, Cat# 230-01101), and S2 subunit (RayBiotech, Cat# 230-01103). The influenza M2e conserved peptide (M2e from human IAV (two copies), avian IAV (one copy), and swine IAV (one copy); 92 aa) was synthesized as previously described [28,42,43]. The mouse-adapted influenza A/Puerto Rico/8/34 (H1N1) strain used for the animal challenge study was generated by reverse genetics as previously described [44]. The replication-competent recombinant vesicular stomatitis virus (rVSVs)-based COVID-19 vaccine v-EM2e/SPΔC1 was generated by inserting the

SP Δ C_{Delta}-I742A gene into the rVSV-E Δ M-M2e vector as described previously [28,42]. The rVSV plasmid V-EM2e/SP Δ C1 was generated by cloning the gene encoding SARS-CoV-2 Delta-SP (SP_{Delta}) containing a C-terminal 17 aa deletion and an I742A point mutation (SP Δ C_{Delta}-I742A or SP Δ C1) into the rVSV-E Δ M-M2e vector (Figure S1) [28,42]. The C-terminus 17 aa deletion facilitates the assembly of SP into the virus, and the I742A point mutation may reduce the SP-mediated infection and syncytia formation [28]. The rVSV-E Δ M-M2e vaccine vector contains an Ebola virus GP protein (EboGP Δ M) fused with the tandem repeats of four copies of influenza M2 ectodomain (24 aa) polypeptide, in which two copies are from human flu strains, one from swine flu strain, and one from avian flu strain [42]. The bivalent rVSV vaccine candidate was rescued in 293T-Vero E6 cocultured cells, propagated, and titrated as described previously [42]. Briefly, the plasmid V-EM2e/SP Δ C1 was transfected into a mix of Vero E6/293T cells together with VSV accessory plasmids encoding P, L, N, and T7 polymerase plasmid. Following the primary transfection, the recovered rVSV was harvested and further amplified in Vero E6 cells. The rVSV in the supernatant was purified and concentrated by ultracentrifugation and then titrated in Vero E6. The necessary amounts of rVSV were diluted with PBS and used for mice immunization experiments.

2.3. Mouse Immunization with rVSV Vaccine v-EM2/SP Δ C1_{Delta}

Oral immunization through the mouse oral cavity was performed by dropping the vaccine (25 μ L/each) in the mouth under the tongue and into the cheek pouches after isoflurane anesthesia and keeping the mouse lying on its side for about 1 min until it woke up [26]. Intranasal immunization was performed also after anesthesia by dropping the vaccine (50 μ L/each) in the nostril. Female BALB/c mice aged 6–8 weeks (five to eight per group) were immunized with bivalent rVSV vaccine v-EM2/SP Δ C1_{Delta} on Day 0 and Day 14 via three different routes: orally (oral/oral, 1×10^6 TCID₅₀), intranasally (i.n./i.n., 1×10^5 TCID₅₀), and combining intranasally at prime and orally at boost (i.n./oral). Immunization with PBS was used as a placebo control. The blood of immunized mice was collected on Day 13 (prime), Day 35 (i.e., 3 weeks post-boost/3 wpB), and Day 49 (5 wpB). These sera were used to measure the RBD-, S2- and M2e-binding antibodies; the neutralizing antibodies; and antibody-dependent cellular cytotoxicity (ADCC).

2.4. Measurement of Vaccine-Induced RBD-, S2-, and M2e-Binding Antibody Titers

To determine RBD-, S2-, and M2e-specific antibodies in mice sera, the sera of immunized mice were $3 \times$ serially diluted in primary antibody diluent (complete RPMI 1640 media with 0.2% (v/v) Tween 20). Enzyme-linked immunosorbent assay (ELISA) 96-well plates (NUNC Maxisorp, Thermo Scientific, Waltham, MA, USA) were coated with recombinant proteins RBD, S2, or M2e (0.75 μ g/mL) in coupling buffer (pH 9.6, 50 mM sodium carbonate-bicarbonate) at 4 $^{\circ}$ C overnight. After blocking at 37 $^{\circ}$ C for 2 h, the ELISA plates were washed and incubated with the diluted sera at 37 $^{\circ}$ C for 1 h. Anti-mouse IgG-HRP antibodies (GE Healthcare, Cat#NA931; 1:5000) were used to detect the antibodies binding to RBD, S2, or M2e. After incubation with the substrate tetramethylbenzidine (TMB) solution (Mandel Scientific, Guelph, ON, Canada) and termination with stop solution, the absorbance at 450 nm (OD₄₅₀) of each well was measured. IgA antibody levels were determined by using the mouse IgA ELISA kit (Thermo fisher, Cat#88-50450-88, Waltham, MA, USA). The endpoint titers of mouse sera were calculated using the interpolation in GraphPad Prism 9.0 with a cutoff of 2.5 times the mean-negative.

2.5. SP Pseudovirus Production and Titration

The SARS-CoV-2 SP-pseudotyped HIV-based luciferase-expressing (Luc) pseudovirus (PV-Luc-SP_{Delta}) was produced by co-transfecting 293T cells in a 6-well plate with the pCAGGS plasmid expressing SP Δ C protein from B.1.617.2 (Delta) [45] (0.5 μ g/well) and a Luc-expressing HIV vector (pNL4-3-R-E-Luc) (1.0 μ g/well), as described previously [28]. The supernatants containing SP-pseudovirus were harvested at 72 h post-transfection,

filtered (0.45 μm filter), aliquoted, and stored at $-80\text{ }^{\circ}\text{C}$. The pseudovirus was titrated on A549_{ACE2} cells by a modified method [28,46,47]. Briefly, the pseudovirus was $2\times$ serially diluted in 25 μL of complete DMEM and mixed with A549_{ACE2} cells (1.25×10^4 /well; 50 μL) and polybrene (5 $\mu\text{g}/\text{mL}$) in a 96-well plate for transduction. After overnight incubation, cells were fed with fresh complete DMEM. At 48–66 h post-infection, cells were lysed in luciferase lysis buffer (Promega; 30 $\mu\text{L}/\text{well}$, Madison, WI, USA), and the luciferase relative light unit (RLU) of the lysates was measured using the luciferase assay system (Promega) and Polerstar optima microplate reader (BMG BioLabtech, Ortenberg, Germany) according to the manufacturer's instructions. The HIV-1 p24 in PVs was also quantified by ELISA, as previously reported [39,40].

2.6. Pseudovirus-Based Neutralization Assays against SARS-CoV-2

The neutralization assay was performed based on SARS-CoV-2 SP-pseudotyped HIV-Luc pseudovirus and A549_{ACE2} cells according to the previous method [28,46,47]. Briefly, $2\times$ serially diluted inactivated mouse sera (starting from 1:50 dilution, 25 μL) was pre-incubated with PV-Luc-SP ΔC (about 10^4 RLU, 25 μL) in complete DMEM with polybrene (5 $\mu\text{g}/\text{mL}$) in a 96-well plate at $37\text{ }^{\circ}\text{C}$ for 1.5 h, then A549_{ACE2} (1.25×10^4 cells/well, 50 μL) was added to each well, and the mixture was incubated at $37\text{ }^{\circ}\text{C}$ for 48 h. The luciferase RLU in cells was measured by using a Luciferase Assay System (Promega). The neutralizing titers or half-maximal inhibitory dilution (ID_{50}) was defined as the reciprocal of the serum maximum dilution that reduced RLU by 50% compared with no-serum (virus and cell) controls. The ID_{50} was calculated by using sigmoid 4PL interpolation with GraphPad Prism 9.0.

2.7. Antibody-Dependent Cellular Cytotoxicity (ADCC) Reporter Assay

The ADCC reporter assay was performed by using Jurkat–Lucia NFAT-CD16 cells (human Fc γ RIII, V158) (Invivogen, Cat# jk1-nfat-cd16) as effector cells according to the manufacturer's instruction with modifications. The engagements among Jurkat–Lucia Fc γ RIII (CD16), antibodies (serum), and antigen-expressing target cells activate luciferase expression driven by NFAT (nuclear factor of activated T cells) in Jurkat–Lucia cells [34,48,49]. In this study, we made use of the ADCC reporter system based on the cross-reactivities of mouse IgG to human Fc γ Rs [48]. Briefly, one day before the assay, 293TN cells (5×10^5 /well, 6-well plate) were transfected with each plasmid expressing SP ΔC of the SARS-CoV-2 Delta variant (1.2 μg DNA) or human influenza A virus M2 (5 μg DNA) using Lipofectamine 3000 (Invitrogen, Waltham, MA, USA) to produce 293TN-S target cells. S expression was semi-quantified by a Western blot the next day (Figures 3A and 4B). The mouse sera were $3\times$ serially diluted in complete DMEM (start from 1:30, 50 $\mu\text{L}/\text{well}$) in a 96-well plate, mixed with target cells 293TN-S or 293TN-M2 (5×10^4 , 50 $\mu\text{L}/\text{well}$), and incubated at $37\text{ }^{\circ}\text{C}$ for 1 h. The Jurkat–Lucia effector cells (1.5×10^5 , 50 $\mu\text{L}/\text{well}$) were added and cultured for an additional 16 h at $37\text{ }^{\circ}\text{C}$ with 5% CO_2 . ADCC activity was determined by measuring the secreted luciferase from activated Jurkat–Lucia cells in the supernatant (30 $\mu\text{L}/\text{well}$). The relative light unit (RLU) was detected by Quanti-Luc substrate solution (25 $\mu\text{L}/\text{well}$, Invivogen) using a Polerstar optima microplate reader (BMG BioLabtech). The background well (only medium) reading was deducted. The no-serum controls were wells containing target cells and Jurkat–Lucia cells. The fold of change (ADCC induction) was calculated as $\text{RLU}(\text{test} - \text{background})/\text{RLU}(\text{no-serum control} - \text{background})$. The ADCC activity of sera was calculated as the geometric mean of the ADCC score (fold change \times dilution factor) from two dilutions.

2.8. Mouse Challenge with Influenza H1N1 Virus PR8

In the influenza virus challenge study, the four groups of female mice (5 for each group) that were immunized with v-EM2/SP $\Delta\text{C}1$ or PBS as described above were intranasally infected with a mouse-adapted strain A/Puerto Rico/8/34 (PR8, H1N1) (3×10^3 PFU/mouse) on Day 42 (4 wpB). The weight and survival of mice were monitored daily for 2 weeks after the challenge. The mice from the PBS group reached the endpoint (moribund or weight

loss over 20%) at 6~7 days post-challenge (1 week post-challenge, 1 wpC), and then were euthanized with two mice of each vaccinated group. The blood/sera and lungs were collected and stored at -80°C for viral load assay, ELISA, and other assays.

2.9. Measurement of Viral Load in the Mouse Lungs (TCID_{50})

To determine the viral load of influenza H1N1 (PR8) in mice, we homogenized each mouse lung in ice-cold 1 mL of DMEM using a tenbroeck glass homogenizer. After spin, the supernatants were $10\times$ serially diluted (starting from $1:10^2$) in the influenza virus infection media (DMEM, 1% P/S, $1\ \mu\text{g}/\text{mL}$ TPCK-trypsin). The inoculums ($100\ \mu\text{L}/\text{well}$) were added into the 96-well plate with 95% confluent MDCK cells and incubated at 37°C . After 3 days, plates were fixed, stained with 2% crystal violet, and scored for cytopathic effect (CPE). The 50% tissue culture infectious dose (TCID_{50}) titers were calculated using a modified Reed and Muench method [50,51].

2.10. Statistical Analysis

Statistical analysis of antibody/cytokine levels was performed using the unpaired Student *t*-test for two groups comparison ($p \geq 0.05$ considered significant) by GraphPad Prism software. The statistical analysis for the endpoint titers, neutralizing antibodies, and mouse weight loss was performed using the one-way ANOVA multiple comparison test followed by Tukey's test with Prism. For the ADCC responses, the two-way ANOVA multiple comparison test followed by Tukey's test was used. For the survival rate, the Log-rank (Mantel-Cox) test was used. The correlation coefficient (r and R^2) and two-tailed p value were calculated via the Pearson method with Prism.

3. Results

3.1. Oral Immunization with v-EM2/SPΔC1_{Delta} Elicited a Robust Humoral Immune Response and Neutralization against SARS-CoV-2 in Mice

Given that the oral deliveries of several rVSV-based vaccines have been reported to induce protective immune responses in animals [25,26], we wanted to extend the vaccination routes of our rVSV-based bivalent vaccine v-EM2/SPΔC1_{Delta} [28] to include oral immunization. To this end, we immunized female BALB/c mice with v-EM2/SPΔC1_{Delta} via oral cavity (oral, 1×10^6 50% tissue culture infectious dose, TCID_{50}) or intranasal (i.n., 1×10^5 TCID_{50}) routes in three groups ($n = 5$ each group) for prime/boost: (1) i.n./i.n.; (2) i.n./oral; and (3) oral/oral (Figure 1A,B). The mice in the control group were given PBS. The interval between prime and booster immunization was 2 weeks. The prime sera (2 weeks post prime) and booster sera (3 weeks post-booster) were collected. Their antibody levels were measured by ELISA (Figures 1 and 2). As expected, intranasal vaccination induced robust anti-SARS-CoV-2 RBD (Figure 1C,E,G) and anti-SARS-CoV-2 S2 (Figure 1D,F) humoral immune responses. Importantly, oral immunization elicited high levels of anti-RBD and anti-S2 IgG, similar to i.n. immunization (Figure 1C–F). The booster significantly enhanced antibody responses in all v-EM2/SPΔC1_{Delta}-immunized groups (Figure 1C,D). Although the oral/oral group showed slightly lower average OD450 values in prime sera, no significant difference was found in the booster sera antibody titers between oral/oral and other immunized groups (Figure 1C–F). However, it is worth mentioning that the dose of oral immunization (10^6 TCID_{50}) was ten times that of i.n. immunization (10^5 TCID_{50}). Moreover, the anti-RBD IgA levels also exhibited high similarity among the three immunized groups (Figure 1G). These findings indicated that mucosal immunization with the v-EM2/SPΔC1_{Delta} vaccine through the oral cavity could effectively induce anti-SARS-CoV-2 SP antibody responses in mice. In addition, we investigated the duration of antibodies in three i.n. immunized mice that were not challenged with the influenza virus. We found the anti-RBD IgG levels in these mice were maintained at a high peak from week 3 to week 5 after the booster (Figure 2A), suggesting that the high levels of anti-SARS-CoV-2 antibodies in mice were sustained during the observed period.

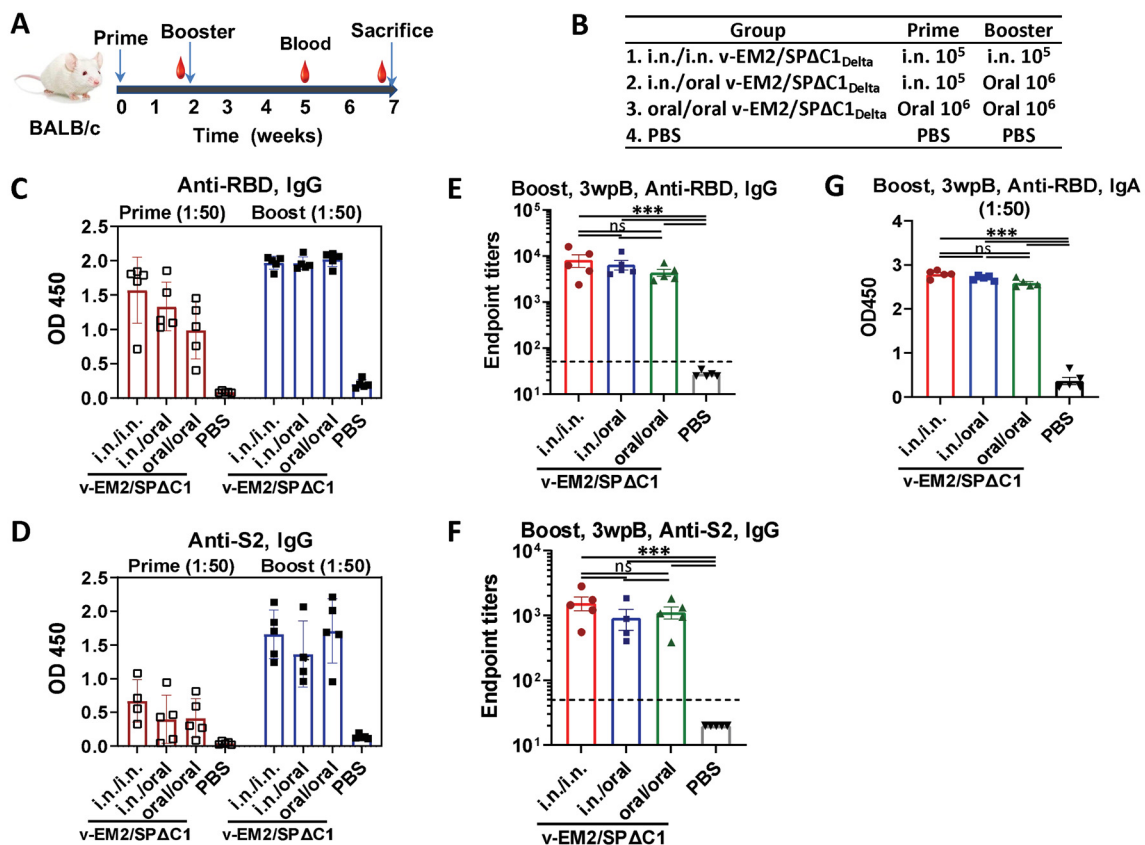


Figure 1. Oral immunization with vaccine candidate v-EM2/SPΔC1_{Delta} elicited robust anti-SARS-CoV-2 RBD and anti-S2 immune response in mice. **(A)** Schematic of the immunization of bivalent rVSV vaccine candidate v-EM2/SPΔC1_{Delta} in mice. BALB/c mice ($n = 5-8$ /group) were immunized with v-EM2/SPΔC1_{Delta} via oral cavity or intranasal routes at weeks 0 and 2, as indicated. The blood from mice in each group was collected on weeks 2 and 5, the mice were sacrificed at week 7 (i.e., 5 weeks post-booster (5 wpB)), and the blood was collected. **(B)** The immunization groups are shown with the delivery route and vaccine dose. **(C–F)** Sera after prime (week 2) and booster (week 5, i.e., 3 weeks post-booster (3 wpB)) immunization were measured for anti-SARS-CoV-2 RBD IgG **(C,E)**, IgA **(G)** levels, and anti-S2 IgG **(D,F)** in OD450 or endpoint titers. Data represent mean \pm SEM. Statistical significance was determined using a one-way ANOVA test and Tukey's test. ***, $p < 0.001$, ns: no significance.

To evaluate if oral immunization with v-EM2/SPΔC1_{Delta} can induce protective immune responses, we measured neutralizing antibody (NAb) levels by using SP_{Delta}-pseudotyped Luciferase+ HIV-based virus particles (PV-Luc-SP_{Delta}) and human angiotensin-converting enzyme 2 (ACE2)-expressing cells A549_{ACE2} [28,39]. The results showed that all three immunized groups induced markedly high NAb titers against the Delta SP-pseudotyped virus in comparison with the control group (Figure 2A). Further, the NAb levels of oral group mice had no significant difference from the other two groups (i.n./i.n. group and i.n./oral group). This finding confirmed that oral immunization with v-EM2/SPΔC1_{Delta} could effectively elicit protective NABs against the SARS-CoV-2 Delta SP-pseudotyped virus at a similar level to the i.n. vaccination. Like the RBD-binding antibodies (Figure 2B), the NAb titers in the i.n. immunized mice sera showed stability from 3 wpB to 5 wpB (Figure 2C), indicating that the high levels of neutralizing antibodies against Delta SP-pseudotyped virus in these immunized mice were sustained during the observed period.

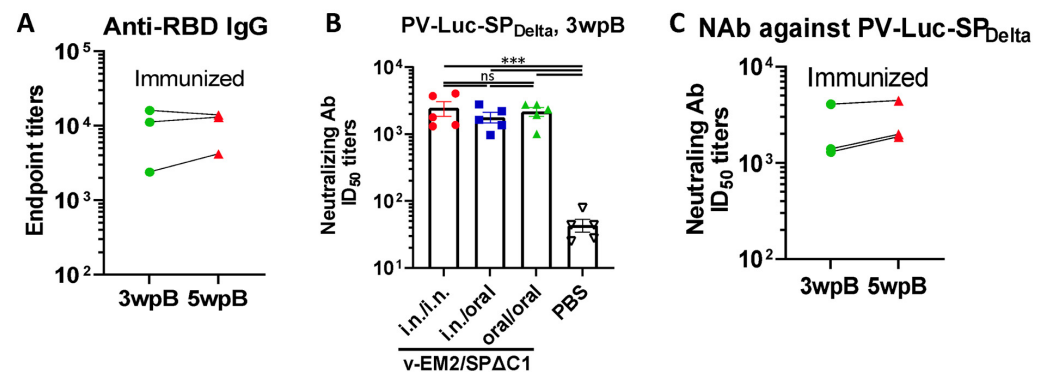


Figure 2. The duration and neutralization of antibodies against SARS-CoV-2 SP induced by oral immunization with v-EM2/SP Δ C1 Δ elta in mice. **(A)** The duration of anti-SARS-CoV-2 RBD (end-point titers) in the i.n. immunized mice sera after booster immunization (3 wpB and 5 wpB) were measured. **(B)** The neutralization titers (50% inhibitory dose, ID₅₀) in immunized mice sera (3 wpB) against pseudovirus PV-Luc-SP Δ elta infection were determined. The serially diluted mouse sera were incubated with PV-Luc-SP Δ elta ($\approx 10^4$ RLU), and then the mixtures (PV + Sera) were used to inoculate A549_{ACE2} cells. The infection of PV was determined by luciferase assay at 48–66 h post-infection. The percentage of infection was calculated compared with the no serum control. The 50% inhibition dose (ID₅₀) neutralizing Ab titers were calculated by using sigmoid 4PL interpolation with GraphPad Prism 9.0, as described in the Materials and Methods. **(C)** The duration of neutralizing Ab ID₅₀ titers in the i.n. immunized mice sera collected at 3 wpB and 5 wpB. Data represent mean \pm SEM. Statistical significance was determined using a one-way ANOVA test and Tukey's test. ***, $p < 0.001$. ns: no significance. wpB, week post-boost.

3.2. Oral Immunization with v-EM2/SP Δ C1 Δ elta Induced ADCC Activities against SARS-CoV-2 in Mice

In addition to neutralization, other immune responses, such as ADCC that can kill virus-infected cells, have been demonstrated to contribute to vaccine protection [34,52]. Therefore, we evaluated the ADCC activity induced by v-EM2/SP Δ C1 Δ elta through a reporter system that used Jurkat–Lucia NFAT (nuclear factor of activated T cells)–CD16 (Invivogen) as effector cells. This T-cell reporter cell line, similar to natural killer (NK) cells, expresses the human Fc receptor Fc γ RIII (CD16; V158 allotype) on the cell surface, which can bind with the Fc region of human IgG and is cross-reactive with the Fc of mouse IgG [48] (Figure 3A, upper panel). If the antibodies are bound with antigen-expressing target cells, the antigen–antibody–Fc γ R engagements will trigger the activation of the NFAT pathway in Jurkat–Lucia cells, including the expression of NFAT-driven reporter luciferase [48,49]. In this study, we used transient expression cells 293TN-SP Δ elta (expressing the SP Δ C of SARS-CoV-2 Delta variant) as target cells (Figure 3A, lower panel, lane 3; Figure S2A). The serially diluted mice sera were first incubated with the target cells 293TN-SP Δ elta, and then the Jurkat–Lucia effector cells were added. ADCC responses were determined by measuring the induction of luciferase secreted from the activated Jurkat–Lucia cells in the supernatants, which were determined via relative light unit (RLU) changes compared to the no-serum control (only target cells and effector cells).

The results revealed that all immunized mice groups had significant ADCC activity against SP Δ elta, with a 23–30 fold change at the first dilution (1:50, log₁₀ dilution = -1.5), compared with the no-serum control (fold change of 1) (Figure 3B). Interestingly, although the oral/oral immunized mice sera showed a slightly lower ADCC activity than other i.n./i.n. and i.n./oral immunized groups, the differences were not statistically significant (Figure 3C), indicating a strong ADCC response was induced by oral immunization with v-EM2/SP Δ C1 Δ elta. In all, these results evidenced that oral vaccination with v-EM2/SP Δ C1 Δ elta in mice elicited remarkable anti-SP Δ elta antibody responses that not only have neutralizing activity but also ADCC activity. Since the mucosa in the nasal cavity and oral cavity are so closely linked to each other, it is reasonable that they have the same efficacy in triggering

host humoral immune responses. Our results indicated that these two immunization routes might be replaceable with each other or be used jointly in some scenarios.

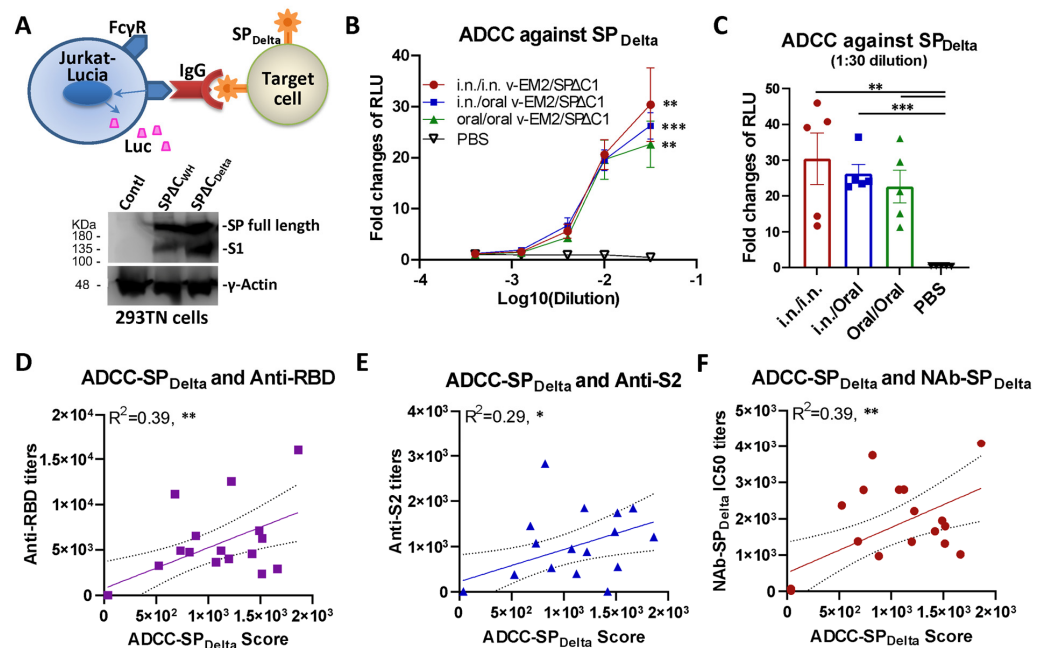


Figure 3. Oral immunization with v-EM2/SP Δ C1 Δ induced the ADCC activities against SARS-CoV-2 SP Δ in mice. (A) The schematic diagram of Jurkat–Lucia-cell-based ADCC activity reporter assay as described in the Materials and Methods. The SP Δ -expressing cells were obtained from transfection and incubated with serially diluted mouse serum (containing SP-binding IgG). Jurkat–Lucia reporter cells expressing Fc γ receptor (Fc γ R) were added to the mixture of SP Δ -expressing cells and serum. The engagement of Fc γ R, IgG, and SP triggered the activation of Jurkat effector cells and the luciferase (Luc) expression. The ADCC activity was determined by measuring the secreted Luc in the cell culture supernatant (upper). The antigen SARS-CoV-2 spike protein (SP Δ _{WH}, SP Δ _{C Δ}) expression in target 293TN cells was determined by Western blotting (lower panel) at 24 h post-transfection using the anti-SARS-CoV-2 SP-NTD (Elabscience, Cat# E-AB-V1030). (B) The ADCC activities against SARS-CoV-2 SP Δ in the immunized mice sera (3 wpB) were determined as described in (A). The ADCC induction (fold change) of sera from each group was calculated against the no-serum control. (C) The ADCC against SP Δ in individual mouse serum at 1:30 dilution. Data represent mean \pm SEM. Statistical significance (B,C) was determined using an ordinary one-way (C) or two-way (B) ANOVA test and Tukey’s test. (D–F) The ADCC activity against SP Δ was positively correlated with the titers of anti-SP antibodies (RBD- or S2-binding) (D,E) or NABs (F) of mice in all groups. The ADCC score was calculated as (fold-change \times dilution factor). The ADCC score geometric mean of the first two dilutions was used. The correlation analysis was performed by Prism. The correlation coefficient (R^2) and two-tailed p -value were calculated via the Pearson method by Prism. *, $p < 0.05$; **, $p < 0.01$; ***, $p < 0.001$.

ADCC is mediated by antigen-bound antibodies that can be recognized and captured by the Fc receptor on effector cells. It is reasonable to assume that only some of the vaccine-induced antibodies can trigger ADCC, so we wanted to know what kind of antibodies have a strong relationship with ADCC. To this end, we investigated the correlation between ADCC activity against SP Δ and the titers of anti-SP antibodies (RBD- or S2-binding) (Figure 3D,E) or NABs (Figure 3F) of mice in all groups. The results showed that ADCC activity against SP Δ was positively correlated with anti-RBD antibodies ($R^2 = 0.39$; **), anti-S2 antibodies ($R^2 = 0.29$; *), and anti-SP Δ NABs ($R^2 = 0.39$; **) (Figure 3D–F). However, these correlations were not strong, suggesting that only a portion of these antibodies are related to ADCC. Similarly, the anti-SP Δ NABs only partially overlapped

with the ADCC-triggering antibodies. Our findings are consistent with previous reports that non-NABs can also induce ADCC [34,38].

3.3. Oral Immunization with v-EM2/SPΔC1_{Delta} Effectively Triggered Humoral Immune Response and ADCC Activity against the Influenza Virus

Given that the bivalent vaccine v-EM2/SPΔC1_{Delta} expresses both SARS-CoV-2 SPΔC1_{Delta} and four copies of the ectodomain of influenza virus M2 protein, we further verified the effectiveness of oral immunization against influenza by detecting anti-M2e IgG in the immunized mice sera (3 wpB) by ELISA. The results showed that the oral/oral immunization route induced a high level of antibodies against M2e, although the level was slightly lower than that of the i.n./i.n. or i.n./oral immunization groups (Figure 4A).

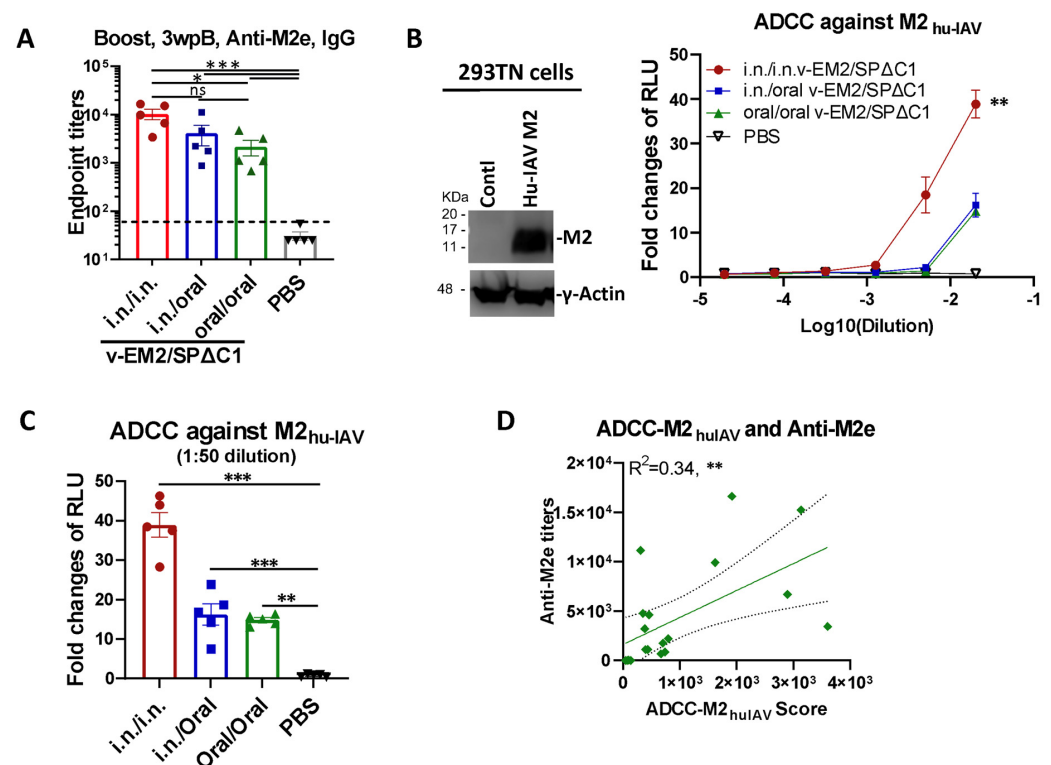


Figure 4. Oral immunization with vaccine candidate v-EM2/SPΔC1_{Delta} effectively triggered a humoral immune response against the influenza virus in mice. (A) The anti-influenza virus matrix-2 (M2) ectodomain (M2e) IgG levels in the sera of the immunized mice at 3 weeks post-booster (3 wpB) as described in Figure 1A were measured by ELISA. (B) The ADCC activities (fold change of RLU) against human influenza virus M2 (M2_{hu-IAV}) in the immunized mice sera (3 wpB) were determined as described in Figure 3A, except using 293TN-M2 target cells. The human influenza A virus (IAV) M2 protein expression in target cells was determined by Western blotting using the sera of mice immunized with v-EM2/ SPΔC1_{Delta} (containing anti-M2 antibodies) (left panel). The ADCC induction (fold change) of serum from each mouse was calculated against the no-serum control (right panel). (C) The ADCC against M2_{hu-IAV} in individual mouse serum at 1:50 dilution. Data represent mean ± SEM. Statistical significance was determined using one-way (A,C) or two-way (B) ANOVA test and Tukey's test. (D) The correlation of ADCC activity against M2_{hu-IAV} and the titers of anti-M2e of mice in all groups. The ADCC score was calculated as described in Figure 3D. The correlation analysis was performed by Prism. The correlation coefficient (R^2) and two-tailed p -value were calculated via the Pearson method. *, $p < 0.05$; **, $p < 0.01$; ***, $p < 0.001$. ns: no significance. wpB, week post-booster.

We then investigated ADCC activity against the human influenza A virus M2 protein (M2_{hu-IAV}) in the mice sera. Briefly, 293TN cells expressing Hu-IVA M2 (Figure 4B, left

panel; Figure S2B) were used as the target cells and incubated with serially diluted mice sera, followed by the addition of Jurkat–Lucia effector cells. ADCC activity was monitored by measuring the induction of luciferase secreted in the supernatants of the mix of 293TN–Hu–IAVM2/Jurkat–Lucia cell cultures (Figure 4B, right panel). The result disclosed that the i.n./i.n.-immunized mice had a significantly higher ADCC activity against M2_{hu-IAV} (fold change of 40 at 1:50 dilution). Further, the oral/oral and i.n./oral immunization sera both showed strong ADCC activity against M2_{hu-IAV} with a 15~16 fold change at 1:50 dilution (Figure 4C). Moreover, we found a positive correlation between the ADCC–M2_{hu-IAV} and the anti-M2e titers ($R^2 = 0.34$, **) (Figure 4D), indicating that a part of anti-M2e antibodies contributed to the ADCC response, as previously reported [53–55]. These results also indicated that ADCC activity in the i.n./oral and oral/oral immunized mice plays an important role in protection against the influenza virus.

3.4. Oral Immunization with v-EM2/SPΔC1_{Delta} Protected Mice from Lethal Influenza Challenge

To investigate the protective effects of oral immunization with v-EM2/SPΔC1_{Delta}, we performed a mouse challenge study by infecting immunized mice with a mouse-adapted influenza A virus PR8 (H1N1). Three different experimental groups of BALB/c mice were immunized with v-EM2/SPΔC1_{Delta} via i.n./i.n, oral/oral, or i.n./oral routes, and a fourth control group was inoculated with PBS. The four groups were then infected with PR8 strain (3000 TCID₅₀/mouse) intranasally on Day 42 (4 wpB) (Figure 5A). Weight loss and survival (Figure 5B) were monitored every day for two weeks following the challenge. Excitingly, we found that the mice of three immunized groups all survived the challenge, indicating that either i.n. or oral immunization, or combined i.n./oral immunization, all effectively protected mice against influenza H1N1 virus infection. This was in contrast to the mice of the control group, which became moribund and reached the endpoint (weight loss of over 20%) within one week (Figure 5B right panel). The immunized mice lost at most 8% of their initial weight at 3 days post-infection (p.i.) and 4 days p.i., and then they gradually regained weight to about 100% within two weeks. Notably, the oral/oral and i.n./oral groups did not show any less protection when compared with the i.n./i.n. group. This result is consistent with the above-described similarity between the anti-M2e antibody levels and the ADCC responses between the i.n. and the oral immunization routes (Figure 4A,C).

The moribund mice in the control group were euthanized, and their blood and lungs were collected. Simultaneously, two mice from each immunized group were also euthanized at 7 days p.i. Their blood and lungs were collected as well. The lung viral loads of these infected mice were determined by TCID₅₀ assay (Figure 5C). The results revealed that all the immunized mice had much lower viral loads in their lungs than the PBS control mice. This finding provides convincing evidence that oral immunization with v-EM2/SPΔC1_{Delta} elicited protective immune responses in mice against influenza as strong as i.n. immunization.

In addition, we were curious as to whether infection with the influenza virus could impact (either enhance or reduce) vaccine-induced immunity against SARS-CoV-2. To answer this question, we measured the anti-RBD IgG titers (Figure 5D) and the NAb titers against SP_{Delta} (Figure 5E) in the sera of mice challenged with influenza PR8 strain and tracked titer changes before (3 wpB) and after challenge (1 and 3 weeks p.i.). The results clearly showed that the levels of anti-RBD IgG and NAb against SP_{Delta} were similar or slightly higher at one week p.i. compared with those before the challenge. However, the anti-RBD IgG and NAb against SP_{Delta} levels returned back at 3wpi. Altogether, the above observations implied that the influenza virus infection did not significantly impact the vaccine-induced immunity against SARS-CoV-2.

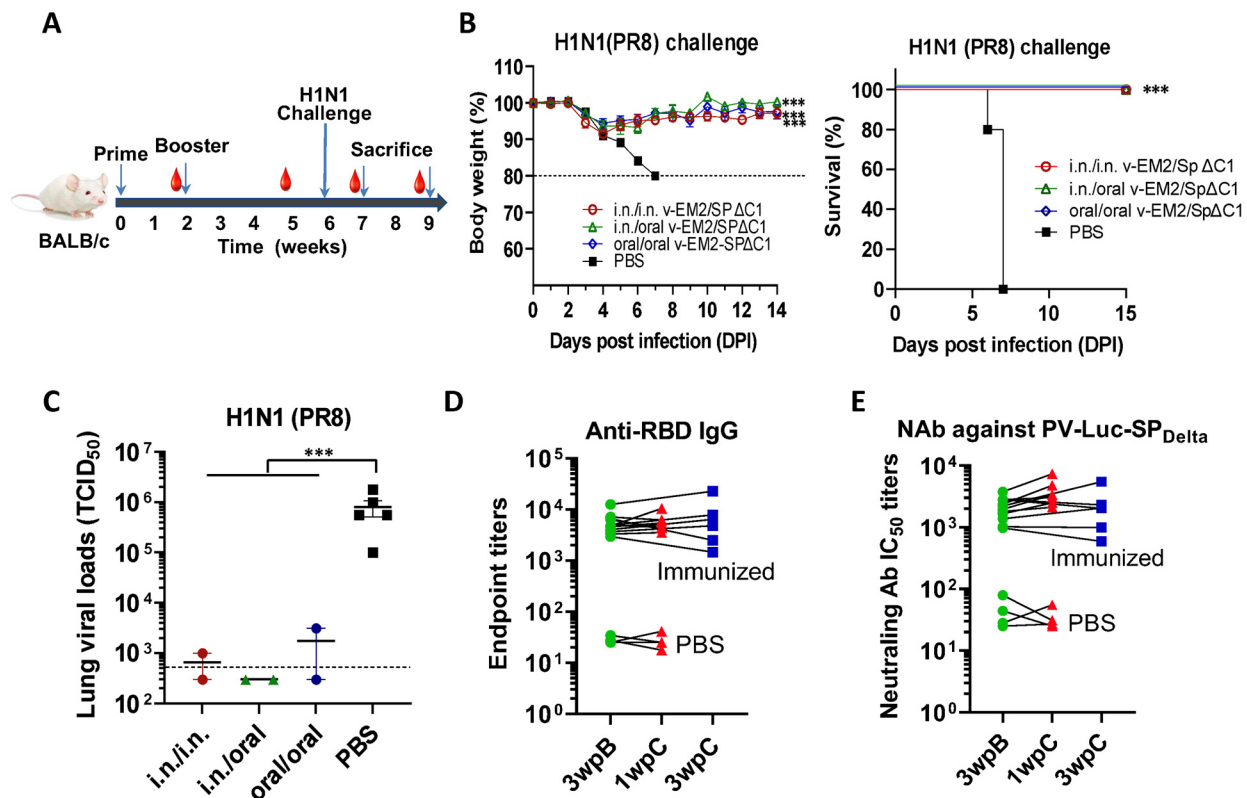


Figure 5. Oral immunization with v-EM2/SPΔC1_{Delta} protected mice from the lethal challenge of H1N1 influenza virus. (A) Schematic of the immunization of bivalent rVSV vaccine v-EM2/SPΔC1_{Delta} and influenza challenge in mice. BALB/c mice (5/group) were immunized with v-EM2/SPΔC1_{Delta} via oral cavity or intranasal routes. At week 6, i.e., 4 weeks post-boost, mice of each group were intranasally infected with the H1N1 influenza virus PR8 (3×10^3 TCID₅₀). Then, the percentages of original body weight ((B), left panel) and survival rates ((B), right panel) of the mice were monitored daily for 2 weeks. (C) Viral loads in the lung tissues of immunized mice (2/group) and PBS group ($n = 5$) at 7 days after H1N1 challenge (1 wpC) were determined with MDCK cells, as described in the Materials and Methods. (D,E) The anti-RBD IgG endpoint titers (D) and NAb titers against PV-Luc-SP_{Delta} in mice sera before (3 wpB) and after challenge (1 wpC and 3 wpC). The titers from the same mouse were linked with a line. Data shown are mean \pm SEM. Statistical significance was determined using unpaired Student's *t*-test (C) or one-way ANOVA test and Tukey's test (A,B) ***, $p < 0.001$. wpB, week post-boost. wpC, week post-challenge. TCID₅₀, 50% tissue culture infectious dose.

4. Discussion

The COVID-19 vaccines approved for emergency use in the last two years can only significantly reduce severe illness and death, but not prevent the virus from spreading [11,12]. The major reason is breakthrough infections caused by immune-escaping SARS-CoV-2 variants. Another possible reason is the weak local immune response triggered by these intramuscularly administered vaccines [5,11,12]. In addition, some evidence indicated that the release of circulating antibodies from the blood to the upper airway mucosa was limited by the restrictive blood–endothelial barrier in mice [56], suggesting the irreplaceable role of the local immune response. Recently, mucosal vaccines have attracted more attention because they efficiently prevent respiratory viral infections by improving the local immune response in addition to systemic responses, as well as reduce barriers to vaccination for people who do not want to get injections [13–16]. In this study, we demonstrated that robust systemic immune responses were induced by oral immunization with an rVSV-based bivalent vaccine (v-EM2/SPΔC1_{Delta}) in mice against the SARS-CoV-2 Delta variant and

H1N1 influenza A virus (IAV). Also, oral immunization with v-EM2/SPΔC1_{Delta} showed efficient protection against H1N1 influenza lethal challenge.

In detail, for the immune responses against SARS-CoV-2 Delta variants, highly similar profiles of anti-RBD and anti-S2 IgG/IgA titers (Figure 1E–G), the anti-SP_{Delta} NAb titers (Figure 2A), and anti-SP_{Delta} ADCC responses (Figure 3B,C) were observed between the oral (10^6 TCID₅₀/dose) and intranasal (10^5 TCID₅₀/dose) routes. Although we did not perform an authentic virus challenge experiment, there is convincing evidence to support the efficacy of oral vaccination. Whether a smaller dose of oral immunization, like 10^5 TCID₅₀, can induce responses of a magnitude close to the i.n. group remains unknown. For the immune responses against influenza A virus, oral immunization achieved complete protection from a lethal H1N1 (PR8) challenge in mice (Figure 5A–C), high levels of anti-M2e antibodies in sera (Figure 4A), and strong anti-M2 ADCC activity (Figure 4B,C).

ADCC is another important anti-viral immune mechanism besides neutralization. Its protective contributions against SARS-CoV-2 [30–34] and influenza [35,36] have been reported. Through ADCC, Fc receptor (FcR)-bearing effector cells (natural killer cells, macrophages, and neutrophils) can recognize and kill target cells that are expressing viral antigens on their surface [34,57,58]. The results provide evidence that oral immunization with our bivalent vaccine (v-EM2/SPΔC1_{Delta}) in mice elicited a strong ADCC response against both the SARS-CoV-2 Delta variant (Figure 3B,C) and influenza virus (Figure 4B,C), suggesting a major contribution of ADCC to protection. The initial step of ADCC is the engagement of Fc receptors on effector cells to specific antibodies that are already bound to the viral antigens on target cells. It is worth noting that the ADCC-inducing antibodies do not need to be neutralizing antibodies [34,38]. Our findings are in line with this: ADCC activity against SP_{Delta} showed a positive correlation with NAb (Figure 3F) but not in a perfect linear relationship, indicating the contribution of non-NABs to ADCC. Another interesting discovery is that ADCC activity was positively correlated with both anti-RBD and anti-S2 antibodies (Figure 3D,E), implying the S1 (RBD) and S2 domains both can induce ADCC antibodies. This result suggests that the presence of both S1 (RBD) and S2 domains in a vaccine may be more beneficial than the single-domain vaccine in triggering ADCC-associated protection.

To our surprise, the ADCC response against influenza-M2e elicited by the oral route was significantly lower than the intranasal group (Figure 4B,C). It appeared to be correlated with the lower anti-M2e levels (Figure 4A). Given the complete protection achieved by both oral and i.n. immunization in the influenza virus challenge study (Figure 5), it seems that such levels of peripheral anti-M2e and/or ADCC-triggering antibodies induced by oral vaccination, especially the local protective immune responses induced (not reported here), are sufficient for protection. However, at this point, we have not investigated if oral immunization with the vaccine could provide equal protection from the SARS-CoV-2 infection, which is warranted for further study.

Our rVSV bivalent vaccine (v-EM2/SPΔC1_{Delta}) is similar to the previously reported VSV-ZEBOV-GP (expressing Zaire Ebolavirus Glycoprotein/GP) vaccine that has been approved for clinical use [19–22]. We replaced the mucin-like domain of ZEBOV-GP with influenza matrix protein 2 ectodomain (M2e) and inserted the SARS-CoV-2 S in the upstream of VSV-L gene [28]. Although Peng et al. recently reported poor immunogenicity for the oral delivery of the vaccine rVSV-SARS2, which expresses a single S protein [26], the difference is that our rVSV vaccine has an EBOV-GPΔM (deletion of the mucin-like domain) that was shown to be able to efficiently facilitate DC and macrophage targeting and induce more potent immune responses [59,60]. Therefore, it is still important to further investigate the mucosal immune response (such as the secreted IgA) and the memory T/B cells in the mucosa. Overall, this study showed successful oral immunization with the rVSV-based vaccine against both influenza and SARS-CoV-2 viral pathogens.

Mucosal vaccines may face the risk of inducing mucosal tolerance (local or systemic immune unresponsiveness) rather than protective immunity [61,62]. Our oral or intranasal vaccination generated significant systemic levels of specific IgG, indicating the rupture

of mucosal tolerance. This may attribute to the replication-competent nature of the rVSV vaccine. In contrast, the oral tablet SARS-CoV-2 vaccine that comprised a non-replicating adenoviral vector elicited protective mucosal IgA but not serum neutralizing antibody in a Phase I clinical trial [14]. In addition, the good manufacturing practices (GMP)-grade VSV-ZEBOV-GP has already been produced for the prevention of Ebola virus disease in humans and also for non-human primate studies [63]. In particular, several GMP-compliant, scalable strategies have been reported to achieve high productivity of rVSV vaccines, such as the single-use bioreactor (SUB) and the serum-free or suspension cell culture techniques [64–66]. The excellent scale-up potential of our rVSV vaccine candidate in manufacture can be expected. In consideration of the efficacy, safety, productivity, and convenience of delivery, oral administration could be a promising option for rVSV-based vaccines, including the v-EM2/SPΔC1_{Delta} vaccine.

In summary, we have demonstrated that oral immunization with the rVSV bivalent vaccine (v-EM2/SPΔC1_{Delta}) in mice induced efficacious immune responses against both SARS-CoV-2 and influenza A virus, including high levels of antibodies that specifically bind to viral antigens and mediate neutralization and ADCC. Further, we also clearly showed that vaccination via an oral route effectively protects mice from influenza virus challenge. As proof of concept, these findings provide evidence of good immunogenicity of the rVSV vaccine v-EM2/SPΔC1_{Delta} delivered in the oral cavity and a high potential to induce protective immune responses.

5. Conclusions

In this study, we investigated the immune response induced by oral immunization with an rVSV bivalent vaccine (v-EM2/SPΔC1_{Delta}) in a mouse model and demonstrated that it was able to elicit strong and protective immune responses, including high levels of antibodies mediating neutralizing and/or antibody-dependent cellular cytotoxicity (ADCC) against SARS-CoV-2 and influenza M2 in mice sera. Furthermore, this vaccine can provide efficient protection against influenza H1N1 virus challenge, with a 100% survival rate and a significantly low lung viral load of virus. All these findings provide substantial evidence for the effectiveness of the rVSV bivalent vaccine through oral delivery.

6. Limitations

The challenge in animals with authentic Delta variant was not included because of the limited availability of a level 4 containment lab. Mucosal immune responses and T/B cell immune responses were not included in this study, so local mucosal immunity induced by oral or nasal routes is still unknown. Our ADCC reporter assay could only detect IgG-induced ADCC, since the Jurkat effector cells express the CD16 (FCγRIII) receptor (IgG Fc receptor), so the data in this study only exhibited IgG-associated ADCC activity, which presented a part of the observed ADCC response, but not the IgA- or IgE-associated ADCC elements.

Supplementary Materials: The following supporting information can be downloaded at: <https://www.mdpi.com/article/10.3390/vaccines11091404/s1>, Figure S1: The diagram of the vaccine candidate rVSV-EM2-SP_{Delta} structure; Figure S2: Expression of SPΔCWT, SPΔCDelta, and Hu-IAV-M2 in 293T cells.

Author Contributions: Conceptualization, X.Y., M.J.O., S.K.P.K., K.R.F. and D.K. The rVSV vaccine preparations were performed by Z.A. and X.Y. Animal immunization and challenge studies, M.J.O. and T.A.O. Neutralization and ADCC experiments, M.J.O., T.A.O. and Z.A. Manuscript writing—review and editing, M.J.O., Z.A., T.A.O., P.L., C.S., S.K.P.K., K.R.F., D.K. and X.Y. Funding acquisition, X.Y., S.K.P.K., K.R.F. and D.K. All authors have read and agreed to the published version of the manuscript.

Funding: This work was supported by the Canadian 2019 Novel Coronavirus (COVID-19) Rapid Research Funding (OV5-170710) by the Canadian Institutes of Health Research (CIHR, cihr-irsc.gc.ca/e/193.html), Research Manitoba (researchmanitoba.ca), and CIHR COVID-19 Variant Supplement grant (VS1-175520) (to X.Y.). This work was also supported by the Manitoba Research Chair Award from Research Manitoba (RM) to X.Y. T.A.O. is a recipient of the University Manitoba Graduate scholarship.

Data Availability Statement: The data sets generated and/or analyzed during the current study are available from the corresponding author.

Conflicts of Interest: The authors declare no conflict of interest.

References

- Andrews, N.; Stowe, J.; Kirsebom, F.; Toffa, S.; Rickeard, T.; Gallagher, E.; Gower, C.; Kall, M.; Groves, N.; O'Connell, A.-M.; et al. COVID-19 Vaccine Effectiveness against the Omicron (B.1.1.529) Variant. *N. Engl. J. Med.* **2022**, *386*, 1532–1546. [[CrossRef](#)] [[PubMed](#)]
- Buchan, S.A.; Chung, H.; Brown, K.A.; Austin, P.C.; Fell, D.B.; Gubbay, J.B.; Nasreen, S.; Schwartz, K.L.; Sundaram, M.E.; Tadrous, M.; et al. Estimated Effectiveness of COVID-19 Vaccines Against Omicron or Delta Symptomatic Infection and Severe Outcomes. *JAMA Netw. Open* **2022**, *5*, e2232760. [[CrossRef](#)] [[PubMed](#)]
- World Health Organization. WHO Coronavirus (COVID-19) Dashboard. 2023. Available online: <https://covid19.who.int/table> (accessed on 15 June 2023).
- Tang, J.; Zeng, C.; Cox, T.M.; Li, C.; Son, Y.M.; Cheon, I.S.; Wu, Y.; Behl, S.; Taylor, J.J.; Chakarabarty, R.; et al. Respiratory mucosal immunity against SARS-CoV-2 after mRNA vaccination. *Sci. Immunol.* **2022**, *7*, eadd4853. [[CrossRef](#)]
- Azzi, L.; Dalla Gasperina, D.; Veronesi, G.; Shallak, M.; Maurino, V.; Baj, A.; Gianfagna, F.; Cavallo, P.; Dentali, F.; Tettamanti, L.; et al. Mucosal immune response after the booster dose of the BNT162b2 COVID-19 vaccine. *eBioMedicine* **2023**, *88*, 104435. [[CrossRef](#)] [[PubMed](#)]
- Huang, N.; Perez, P.; Kato, T.; Mikami, Y.; Okuda, K.; Gilmore, R.C.; Conde, C.D.; Gasmi, B.; Stein, S.; Beach, M.; et al. SARS-CoV-2 infection of the oral cavity and saliva. *Nat. Med.* **2021**, *27*, 892–903. [[CrossRef](#)] [[PubMed](#)]
- Killingley, B.; Nguyen-Van-Tam, J. Routes of influenza transmission. *Influenza Other Respir. Viruses* **2013**, *7* (Suppl. S2), 42–51. [[CrossRef](#)] [[PubMed](#)]
- Krammer, F. The human antibody response to influenza A virus infection and vaccination. *Nat. Rev. Immunol.* **2019**, *19*, 383–397.
- Mao, T.; Israelow, B.; Suberi, A.; Zhou, L.; Reschke, M.; Peña-Hernández, M.A.; Dong, H.; Homer, R.J.; Saltzman, W.M.; Iwasaki, A. Unadjuvanted intranasal spike vaccine booster elicits robust protective mucosal immunity against sarbecoviruses. *bioRxiv* **2022**. [[CrossRef](#)]
- Le Nouën, C.; Nelson, C.E.; Liu, X.; Park, H.-S.; Matsuoka, Y.; Luongo, C.; Santos, C.; Yang, L.; Herbert, R.; Castens, A.; et al. Intranasal pediatric parainfluenza virus-vectored SARS-CoV-2 vaccine candidate is protective in macaques. *bioRxiv* **2022**. [[CrossRef](#)]
- Waltz, E. China and India approve nasal COVID vaccines—Are they a game changer? *Nature* **2022**, *609*, 450. [[CrossRef](#)]
- Waltz, E. How nasal-spray vaccines could change the pandemic. *Nature* **2022**, *609*, 240–242. [[CrossRef](#)] [[PubMed](#)]
- Kar, S.; Devnath, P.; Emran, T.B.; Tallei, T.E.; Mitra, S.; Dhama, K. Oral and intranasal vaccines against SARS-CoV-2: Current progress, prospects, advantages, and challenges. *Immun. Inflamm. Dis.* **2022**, *10*, e604. [[CrossRef](#)] [[PubMed](#)]
- Johnson, S.; Martinez, C.I.; Jegede, C.B.; Gutierrez, S.; Cortese, M.; Martinez, C.J.; Garg, S.J.; Peinovich, N.; Dora, E.G.; Tucker, S.N. SARS-CoV-2 oral tablet vaccination induces neutralizing mucosal IgA in a phase 1 open label trial. *medRxiv* **2022**. [[CrossRef](#)]
- Li, J.-X.; Wu, S.-P.; Guo, X.-L.; Tang, R.; Huang, B.-Y.; Chen, X.-Q.; Chen, Y.; Hou, L.-H.; Liu, J.-X.; Zhong, J.; et al. Safety and immunogenicity of heterologous boost immunisation with an orally administered aerosolised Ad5-nCoV after two-dose priming with an inactivated SARS-CoV-2 vaccine in Chinese adults: A randomised, open-label, single-centre trial. *Lancet Respir. Med.* **2022**, *10*, 739–748. [[CrossRef](#)] [[PubMed](#)]
- Jin, L.; Tang, R.; Wu, S.; Guo, X.; Hou, L.; Chen, X.; Zhu, T.; Gou, J.; Huang, H.; Zhong, J.; et al. Antibody Persistence and Safety through 6 Months after Heterologous Orally Aerosolised Ad5-nCoV in individuals primed with two-dose CoronaVac previously. *medRxiv* **2022**. [[CrossRef](#)]
- Banihashemi, S.R.; Es-Haghi, A.; Fallah Mehrabadi, M.H.; Nofeli, M.; Mokarram, A.R.; Ranjbar, A.; Salman, M.; Hajimoradi, M.; Razaz, S.H.; Taghdiri, M.; et al. Safety and Efficacy of Combined Intramuscular/Intranasal RAZI-COV PARS Vaccine Candidate Against SARS-CoV-2: A Preclinical Study in Several Animal Models. *Front. Immunol.* **2022**, *13*, 836745. [[CrossRef](#)]
- Fathi, A.; Dahlke, C.; Addo, M.M. Recombinant vesicular stomatitis virus vector vaccines for WHO blueprint priority pathogens. *Hum. Vaccines Immunother.* **2019**, *15*, 2269–2285. [[CrossRef](#)]
- Suder, E.; Furuyama, W.; Feldmann, H.; Marzi, A.; de Wit, E. The vesicular stomatitis virus-based Ebola virus vaccine: From concept to clinical trials. *Hum. Vaccines Immunother.* **2018**, *14*, 2107–2113. [[CrossRef](#)]
- Pinski, A.N.; Messaoudi, I. Therapeutic vaccination strategies against EBOV by rVSV-EBOV-GP: The role of innate immunity. *Curr. Opin. Virol.* **2021**, *51*, 179–189. [[CrossRef](#)]

21. Jones, S.M.; Ströher, U.; Fernando, L.; Qiu, X.; Alimonti, J.; Melito, P.; Bray, M.; Klenk, H.-D.; Feldmann, H. Assessment of a Vesicular Stomatitis Virus-Based Vaccine by Use of the Mouse Model of Ebola Virus Hemorrhagic Fever. *J. Infect. Dis.* **2007**, *196*, S404–S412. [[CrossRef](#)]
22. Geisbert, T.W.; Daddario-DiCaprio, K.M.; Lewis, M.G.; Geisbert, J.B.; Grolla, A.; Leung, A.; Paragas, J.; Matthias, L.; Smith, M.A.; Jones, S.M.; et al. Vesicular Stomatitis Virus-Based Ebola Vaccine Is Well-Tolerated and Protects Immunocompromised Nonhuman Primates. *PLoS Pathog.* **2008**, *4*, e1000225. [[CrossRef](#)] [[PubMed](#)]
23. Choi, M.J.; Cossaboom, C.M.; Whitesell, A.N.; Dyal, J.W.; Joyce, A.; Morgan, R.L.; Campos-Outcalt, D.; Person, M.; Ervin, E.; Yu, Y.C.; et al. Use of Ebola Vaccine: Recommendations of the Advisory Committee on Immunization Practices, United States, 2020. *MMWR Recomm. Rep.* **2021**, *70*, 1–12. [[CrossRef](#)] [[PubMed](#)]
24. Durrant, D.M.; Ghosh, S.; Klein, R.S. The Olfactory Bulb: An Immunosensory Effector Organ during Neurotropic Viral Infections. *ACS Chem. Neurosci.* **2016**, *7*, 464–469. [[CrossRef](#)] [[PubMed](#)]
25. Warner, B.M.; Jangra, R.K.; Griffin, B.D.; Stein, D.R.; Kobasa, D.; Chandran, K.; Kobinger, G.P.; Safronetz, D. Oral Vaccination with Recombinant Vesicular Stomatitis Virus Expressing Sin Nombre Virus Glycoprotein Prevents Sin Nombre Virus Transmission in Deer Mice. *Front. Cell. Infect. Microbiol.* **2020**, *10*, 333. [[CrossRef](#)]
26. Peng, K.W.; Carey, T.; Lech, P.; Vandergaast, R.; Muñoz-Alía, M.; Packiriswamy, N.; Gnanadurai, C.; Krotova, K.; Tesfay, M.; Ziegler, C.; et al. Boosting of SARS-CoV-2 immunity in nonhuman primates using an oral rhabdoviral vaccine. *Vaccine* **2022**, *40*, 2342–2351. [[CrossRef](#)]
27. Kleinfelder, L.M.; Jangra, R.K.; Jae, L.T.; Herbert, A.S.; Mittler, E.; Stiles, K.M.; Wirchnianski, A.S.; Kielian, M.; Brummelkamp, T.R.; Dye, J.M.; et al. Haploid Genetic Screen Reveals a Profound and Direct Dependence on Cholesterol for Hantavirus Membrane Fusion. *mBio* **2015**, *6*, e00801-15. [[CrossRef](#)]
28. Ao, Z.; Ouyang, M.J.; Olukitibi, T.A.; Warner, B.; Vendramelli, R.; Truong, T.; Meilleur, C.; Zhang, M.; Kung, S.; Fowke, K.R.; et al. A Recombinant VSV-Based Bivalent Vaccine Effectively Protects against Both SARS-CoV-2 and Influenza A Virus Infection. *J. Virol.* **2022**, *96*, e0133722. [[CrossRef](#)]
29. Zohar, T.; Alter, G. Dissecting antibody-mediated protection against SARS-CoV-2. *Nat. Rev. Immunol.* **2020**, *20*, 392–394. [[CrossRef](#)]
30. Vigón, L.; García-Pérez, J.; Rodríguez-Mora, S.; Torres, M.; Mateos, E.; Castillo de la Osa, M.; Cervero, M.; Malo De Molina, R.; Navarro, C.; Murciano-Antón, M.A.; et al. Impaired Antibody-Dependent Cellular Cytotoxicity in a Spanish Cohort of Patients with COVID-19 Admitted to the, I.C.U. *Front. Immunol.* **2021**, *12*, 742631. [[CrossRef](#)]
31. Tso, F.Y.; Lidenge, S.J.; Poppe, L.K.; Pena, P.B.; Privatt, S.R.; Bennett, S.J.; Ngowi, J.R.; Mwaiselage, J.; Belshan, M.; Siedlik, J.A.; et al. Presence of antibody-dependent cellular cytotoxicity (ADCC) against SARS-CoV-2 in COVID-19 plasma. *PLoS ONE* **2021**, *16*, e0247640. [[CrossRef](#)]
32. Hagemann, K.; Riecken, K.; Jung, J.M.; Hildebrandt, H.; Menzel, S.; Bunders, M.J.; Fehse, B.; Koch-Nolte, F.; Heinrich, F.; Peine, S.; et al. Natural killer cell-mediated ADCC in SARS-CoV-2-infected individuals and vaccine recipients. *Eur. J. Immunol.* **2022**, *52*, 1297–1307. [[CrossRef](#)] [[PubMed](#)]
33. Cui, T.; Huang, M.; Su, X.; Lin, Z.; Zhong, J.; Yang, X.; Wang, Z. Potential of Antibody-Dependent Cellular Cytotoxicity in Acute and Recovery Phases of SARS-CoV-2 Infection. *Infect. Dis. Immun.* **2022**, *2*, 74–82. [[CrossRef](#)]
34. Yu, Y.; Wang, M.; Zhang, X.; Li, S.; Lu, Q.; Zeng, H.; Hou, H.; Li, H.; Zhang, M.; Jiang, F.; et al. Antibody-dependent cellular cytotoxicity response to SARS-CoV-2 in COVID-19 patients. *Signal Transduct. Target. Ther.* **2021**, *6*, 346. [[CrossRef](#)] [[PubMed](#)]
35. Gao, R.; Sheng, Z.; Sreenivasan, C.C.; Wang, D.; Li, F. Influenza A Virus Antibodies with Antibody-Dependent Cellular Cytotoxicity Function. *Viruses* **2020**, *12*, 276. [[CrossRef](#)] [[PubMed](#)]
36. Von Holle, T.A.; Moody, M.A. Influenza and Antibody-Dependent Cellular Cytotoxicity. *Front. Immunol.* **2019**, *10*, 1457. [[CrossRef](#)]
37. Bournazos, S.; Klein, F.; Pietzsch, J.; Seaman, M.S.; Nussenzweig, M.C.; Ravetch, J.V. Broadly neutralizing anti-HIV-1 antibodies require Fc effector functions for in vivo activity. *Cell* **2014**, *158*, 1243–1253. [[CrossRef](#)]
38. Liu, Q.; Fan, C.; Li, Q.; Zhou, S.; Huang, W.; Wang, L.; Sun, C.; Wang, M.; Wu, X.; Ma, J.; et al. Antibody-dependent-cellular-cytotoxicity-inducing antibodies significantly affect the post-exposure treatment of Ebola virus infection. *Sci. Rep.* **2017**, *7*, 45552. [[CrossRef](#)]
39. Ao, Z.; Ouyang, M.J.; Olukitibi, T.A.; Yao, X. SARS-CoV-2 Delta spike protein enhances the viral fusogenicity and inflammatory cytokine production. *iScience* **2022**, *25*, 104759. [[CrossRef](#)]
40. Ouyang, M.J.; Ao, Z.; Olukitibi, T.A.; Yao, X.J. Protocol to evaluate the inflammatory response in human macrophages induced by SARS-CoV-2 spike-pseudotyped VLPs. *STAR Protoc.* **2023**, *4*, 102083. [[CrossRef](#)]
41. Ao, Z.; Patel, A.; Tran, K.; He, X.; Fowke, K.; Coombs, K.; Kobasa, D.; Kobinger, G.; Yao, X. Characterization of a trypsin-dependent avian influenza H5N1-pseudotyped HIV vector system for high throughput screening of inhibitory molecules. *Antivir. Res.* **2008**, *79*, 12–18. [[CrossRef](#)]
42. Olukitibi, T.; Ao, Z.-j.; Azizi, H.; Mahmoudi, M.; Coombs, K.; Kobasa, D.; Kobinger, G.; Yao, X.-J. Development and characterization of influenza M2 ectodomain and/or HA stalk-based DC-targeting vaccines for different influenza infections. *Front. Microbiol.* **2022**, *13*, 937192. [[CrossRef](#)]
43. Liu, W.; Zou, P.; Ding, J.; Lu, Y.; Chen, Y.-H. Sequence comparison between the extracellular domain of M2 protein human and avian influenza A virus provides new information for bivalent influenza vaccine design. *Microbes Infect.* **2005**, *7*, 171–177. [[CrossRef](#)]

44. Ranadheera, C.; Coombs, K.M.; Kobasa, D. Comprehending a Killer: The Akt/mTOR Signaling Pathways Are Temporally High-Jacked by the Highly Pathogenic 1918 Influenza Virus. *EBioMedicine* **2018**, *32*, 142–163. [[CrossRef](#)]
45. Mlcochova, P.; Kemp, S.A.; Dhar, M.S.; Papa, G.; Meng, B.; Ferreira, I.A.T.M.; Datt, R.; Collier, D.A.; Albecka, A.; Singh, S.; et al. SARS-CoV-2 B.1.617.2 Delta variant replication and immune evasion. *Nature* **2021**, *599*, 114–119. [[CrossRef](#)]
46. Donofrio, G.; Franceschi, V.; Macchi, F.; Russo, L.; Rocci, A.; Marchica, V.; Costa, F.; Giuliani, N.; Ferrari, C.; Missale, G. A Simplified SARS-CoV-2 Pseudovirus Neutralization Assay. *Vaccines* **2021**, *9*, 389. [[CrossRef](#)]
47. Hu, J.; Gao, Q.; He, C.; Huang, A.; Tang, N.; Wang, K. Development of cell-based pseudovirus entry assay to identify potential viral entry inhibitors and neutralizing antibodies against SARS-CoV-2. *Genes Dis.* **2020**, *7*, 551–557. [[CrossRef](#)]
48. Temming, A.R.; Bentlage, A.E.H.; de Taeye, S.W.; Bosman, G.P.; Lissenberg-Thunnissen, S.N.; Derksen, N.I.L.; Brassier, G.; Mok, J.Y.; van Esch, W.J.E.; Howie, H.L.; et al. Cross-reactivity of mouse IgG subclasses to human Fc gamma receptors: Antibody deglycosylation only eliminates IgG2b binding. *Mol. Immunol.* **2020**, *127*, 79–86. [[CrossRef](#)]
49. Cao, J.; Wang, L.; Yu, C.; Wang, K.; Wang, W.; Yan, J.; Li, Y.; Yang, Y.; Wang, X.; Wang, J. Development of an antibody-dependent cellular cytotoxicity reporter assay for measuring anti-Middle East Respiratory Syndrome antibody bioactivity. *Sci. Rep.* **2020**, *10*, 16615. [[CrossRef](#)]
50. Karakus, U.; Cramer, M.; Lanz, C.; Yángüez, E. Propagation and Titration of Influenza Viruses. In *Influenza Virus: Methods and Protocols*; Yamauchi, Y., Ed.; Springer: New York, NY, USA, 2018; pp. 59–88. [[CrossRef](#)]
51. Reed, L.J.; Muench, H. A simple method of estimating fifty percent endpoints. *Am. J. Epidemiol.* **1938**, *27*, 493–497. [[CrossRef](#)]
52. Lee, W.S.; Selva, K.J.; Davis, S.K.; Wines, B.D.; Reynaldi, A.; Esterbauer, R.; Kelly, H.G.; Haycroft, E.R.; Tan, H.X.; Juno, J.A.; et al. Decay of Fc-dependent antibody functions after mild to moderate COVID-19. *Cell Rep. Med.* **2021**, *2*, 100296. [[CrossRef](#)]
53. Simhadri, V.R.; Dimitrova, M.; Mariano, J.L.; Zenarruzabeitia, O.; Zhong, W.; Ozawa, T.; Muraguchi, A.; Kishi, H.; Eichelberger, M.C.; Borrego, F. A Human Anti-M2 Antibody Mediates Antibody-Dependent Cell-Mediated Cytotoxicity (ADCC) and Cytokine Secretion by Resting and Cytokine-Preactivated Natural Killer (NK) Cells. *PLoS ONE* **2015**, *10*, e0124677. [[CrossRef](#)] [[PubMed](#)]
54. Wang, R.; Song, A.; Levin, J.; Dennis, D.; Zhang, N.J.; Yoshida, H.; Koriazova, L.; Madura, L.; Shapiro, L.; Matsumoto, A.; et al. Therapeutic potential of a fully human monoclonal antibody against influenza A virus M2 protein. *Antivir. Res.* **2008**, *80*, 168–177. [[CrossRef](#)] [[PubMed](#)]
55. El Bakkouri, K.; Descamps, F.; De Filette, M.; Smet, A.; Festjens, E.; Birkett, A.; Van Rooijen, N.; Verbeek, S.; Fiers, W.; Saelens, X. Universal vaccine based on ectodomain of matrix protein 2 of influenza A: Fc receptors and alveolar macrophages mediate protection. *J. Immunol.* **2011**, *186*, 1022–1031. [[CrossRef](#)] [[PubMed](#)]
56. Wellford, S.A.; Moseman, A.P.; Dao, K.; Wright, K.E.; Chen, A.; Plevin, J.E.; Liao, T.-C.; Mehta, N.; Moseman, E.A. Mucosal plasma cells are required to protect the upper airway and brain from infection. *Immunity* **2022**, *55*, 2118–2134.e6. [[CrossRef](#)]
57. Su, B.; Dispinseri, S.; Iannone, V.; Zhang, T.; Wu, H.; Carapito, R.; Bahram, S.; Scarlatti, G.; Moog, C. Update on Fc-Mediated Antibody Functions Against HIV-1 Beyond Neutralization. *Front. Immunol.* **2019**, *10*, 2968. [[CrossRef](#)]
58. Tauzin, A.; Nayrac, M.; Benlarbi, M.; Gong, S.Y.; Gasser, R.; Beaudoin-Bussièrès, G.; Brassard, N.; Laumaea, A.; Vézina, D.; Prévost, J.; et al. A single dose of the SARS-CoV-2 vaccine BNT162b2 elicits Fc-mediated antibody effector functions and T cell responses. *Cell Host Microbe* **2021**, *29*, 1137–1150.e6. [[CrossRef](#)]
59. Ao, Z.; Wang, L.; Mendoza, E.J.; Cheng, K.; Zhu, W.; Cohen, E.A.; Fowke, K.; Qiu, X.; Kobinger, G.; Yao, X. Incorporation of Ebola glycoprotein into HIV particles facilitates dendritic cell and macrophage targeting and enhances HIV-specific immune responses. *PLoS ONE* **2019**, *14*, e0216949. [[CrossRef](#)]
60. Olukitibi, T.A.; Ao, Z.; Mahmoudi, M.; Kobinger, G.A.; Yao, X. Dendritic cells/macrophages targeting feature of Ebola glycoprotein and its potential as immunological facilitator for antiviral vaccine approach. *Microorganisms* **2019**, *7*, 402. [[CrossRef](#)]
61. Russell, M.W.; Mestecky, J. Mucosal immunity: The missing link in comprehending SARS-CoV-2 infection and transmission. *Front. Immunol.* **2022**, *13*, 957107. [[CrossRef](#)]
62. Chistiakov, D.A.; Bobryshev, Y.V.; Kozarov, E.; Sobenin, I.A.; Orekhov, A.N. Intestinal mucosal tolerance and impact of gut microbiota to mucosal tolerance. *Front. Microbiol.* **2014**, *5*, 781. [[CrossRef](#)]
63. Marzi, A.; Robertson, S.J.; Haddock, E.; Feldmann, F.; Hanley, P.W.; Scott, D.P.; Strong, J.E.; Kobinger, G.; Best, S.M.; Feldmann, H. EBOLA VACCINE. VSV-EBOV rapidly protects macaques against infection with the 2014/15 Ebola virus outbreak strain. *Science* **2015**, *349*, 739–742. [[CrossRef](#)] [[PubMed](#)]
64. Ton, C.; Stabile, V.; Carey, E.; Maraïkar, A.; Whitmer, T.; Marrone, S.; Afanador, N.L.; Zabrodin, I.; Manomohan, G.; Whiteman, M.; et al. Development and scale-up of rVSV-SARS-CoV-2 vaccine process using single use bioreactor. *Biotechnol. Rep.* **2023**, *37*, e00782. [[CrossRef](#)] [[PubMed](#)]
65. Bakhshizadeh Gashti, A.; Chahal, P.S.; Gaillet, B.; Garnier, A. Purification of recombinant vesicular stomatitis virus-based HIV vaccine candidate. *Vaccine* **2023**, *41*, 2198–2207. [[CrossRef](#)] [[PubMed](#)]
66. Gelinas, J.F.; Azizi, H.; Kiesslich, S.; Lanthier, S.; Perderson, J.; Chahal, P.S.; Ansoerge, S.; Kobinger, G.; Gilbert, R.; Kamen, A.A. Production of rVSV-ZEBOV in serum-free suspension culture of HEK 293SF cells. *Vaccine* **2019**, *37*, 6624–6632. [[CrossRef](#)] [[PubMed](#)]

Disclaimer/Publisher’s Note: The statements, opinions and data contained in all publications are solely those of the individual author(s) and contributor(s) and not of MDPI and/or the editor(s). MDPI and/or the editor(s) disclaim responsibility for any injury to people or property resulting from any ideas, methods, instructions or products referred to in the content.